DR SEAN CURTIS JONES (Orcid ID : 0000-0003-4569-7297)

PROFESSOR BARRY KOHN (Orcid ID : 0000-0001-5064-5454)

Article type : Special issue - Thermo2018

Received date: 19-Nov-2018
Revised version received date: 25-Jan-2019
Accepted date: 12-Feb-2019

Correspondence to:
Dr Sean Jones



# *Special issue - Thermo2018*

# Etching of Fission Tracks in Monazite: An Experimental Study

**Short Title: Experimental Etching of Fission Tracks in Monazite**

*Sean Jones[1], Andy Gleadow[1], Barry Kohn[1], Steven M. Reddy[2]*

1. Department of Earth Sciences, University of Melbourne, Melbourne 3000, Australia
2. School of Earth and Planetary Sciences, Curtin University, Bentley 6102, Australia

Sean Jones
Tel: +61 3 8344 7675
Email address: seanj1@student.unimelb.edu.au
ORCID ID: 0000-0003-4569-7297

Andrew Gleadow
Tel: +61 3 8344 5700
Email Address: gleadow@unimelb.edu.au
ORCID ID: 0000-0003-0496-0028

Barry Kohn
Tel: +61 3 8344 7217
Email Address: b.kohn@unimelb.edu.au
ORCID: 0000-0001-5064-5454

Steven Reddy
Tel: +61 8 9266 4371
Fax: +61 8 9266 3153
Email Address: s.reddy@curtin.edu.au
ORCID: 0000-0002-4726-5714

*Footnote: This paper was presented at the 16th International Conference on Thermochronology (Quedlinburg, Germany, September 2018)*

***Abstract***

This study reports a range of etching and annealing experiments to establish the optimum conditions for the etching of fission tracks in monazite. The previously reported concentrated (12M) HCl etchant at 90°C, was found to cause grain loss from epoxy mounts and high degrees of grain corrosion, as did much longer etching times at lower temperatures. Using implanted $^{252}$Cf semi-tracks, a series of experiments were performed on internal prismatic faces of monazite-(Ce) crystals from the Paleozoic Harcourt Granodiorite (Victoria, Australia) using an alternative 6M HCl etchant, also at 90°C. Step-etch results show optimal etching at 60-90 minutes. Further, an isothermal annealing experiment, illustrated that the degree of annealing that can be expected during etching at 90°C under laboratory timescales is negligible. The etching rate between grains is not uniform, with a correlation demonstrated between over-etched grains and high U and Th concentrations.

### *1. Introduction*

Monazite ((Ce, La, Nd, Sm)$PO_4$), a rare earth (RE) bearing phosphate, is commonly found as an accessory mineral in igneous, metamorphic and vein rocks. Resistance to weathering and abrasion also makes this mineral a common detrital phase in the heavy mineral fraction of clastic sedimentary rocks (e.g. Nesse, 2012).

The common occurrence of monazite, containing significant uranium (U) and thorium (Th), makes it a useful mineral for isotopic and chemical dating. While the U-Th-Pb and (U-Th)/He dating systems (e.g. Cottle *et al.,* 2009 and Peterman *et al.,* 2014) have both been developed, only limited investigations have been undertaken as to its potential for fission track dating. A critical first-step towards developing monazite fission track thermochronology is establishing the optimum fission-track etching conditions (e.g. Gleadow *et al.,* 2002). Shukoljukov and Komarov (1970) reported the first known etching method for monazite using concentrated (37%, 12M) HCl at 90°C for 45 minutes. Since that work however, little progress has been made in further investigating monazite etching properties. Fayon (2011) reported differences in fission-track etching efficiencies that could possibly be attributed to U content (i.e. lower U content required longer etching times). Weise *et al.,* (2009) reported a monazite annealing study based on the implantation of Kr heavy ion tracks, using concentrated HCl at 50°C for 18 hours. This lower temperature was used due to the prediction that fission tracks in monazite are likely to anneal at lower temperatures than in apatite (Gleadow *et al.,* 2004, 2005; Shipley & Fayon, 2006).

Although the original concentrated HCl protocol etches clear fission tracks, a significant problem is the highly corrosive nature of the etchant. After 45 minutes, grains may be corroded such that fission tracks are difficult to observe and grain loss from the epoxy mount becomes common (Figure 1). This study aims to explore alternative etchants under varying concentrations and temperatures, particularly to assess whether tracks can be etched effectively at lower temperatures or concentrations to minimise grain loss.

------------------------------------- Figure 1 hereabouts ------------------------------------

### *2. Experiments and Results*

Euhedral monazite-(Ce) crystals (~100-250 µm in length) from the late Devonian Harcourt Granodiorite (Victoria, Australia) were used in this study. This is a high-K, calc-alkaline granite dated by zircon U-Pb at ~370 Ma (Clemens, 2018). Grains were mounted in epoxy and polished using standard procedures (e.g. Kohn et al, 2018). Different acid and alkali etchants were tested including: HF (40%), HF (40%) : $HNO_3$ (34.81%) : HCl (37%) : $H_2O$ (1:2:3:6 by volume), 98% $H_2SO_4$, $H_2SO_4$ (98%) : HCl (37%) : $H_2O$ (1:1:1 by volume), $HNO_3$ (34.81%) and NaOH (0.52% and 4%) (see Fleischer et al, 1975; Wagner & Van den Haute, 1992 for different etchant lists). Most of these experiments were conducted at room temperature but none successfully etched tracks, even for up to 10 hours. After further experiments with HCl at various concentrations and temperatures, it was concluded that a 6M HCl (HCl (37%) : $H_2O$ (1:1 by volume)) solution at 90°C reduced both grain corrosion and grain loss from the epoxy mount, while typically etching fission tracks within 1-2 hours.

### *2.1 Electron Backscatter Diffraction*

Electron Backscatter Diffraction (EBSD), a microstructural characterization technique used to analyze the structure and crystal orientation of minerals (e.g. Prior *et al.,* 1999), was carried out to determine the dominant orientation at which monazite crystals settle when being prepared for fission-track etching using standard mounting techniques (see Kohn *et al.,* 2019). Analyses were carried out at the Microscopy and Microanalysis Facility, Curtin University, as described by Erikson et al. (2015), on two different mounts of Harcourt monazite grains. The hypothesis tested was that euhedral grains would fall on their {100} prismatic faces, which would ensure consistency in experiments and routine fission-track dating. Analysis of grains of similar orientation is important as different crystallographic orientations in monazite could have varying etching characteristics. Individual crystal orientation measurements are shown in Figure 2 and show strongly preferred orientations with the {100} plane lying parallel to the mounting substrate in 26 of 33 monazite crystals (across both mounts). These measurements strongly suggest that monazite grains retaining their crystal morphology will predominantly be oriented on their {100} prismatic faces during mounting.

------------------------------------ Figure 2 hereabouts ------------------------------------

### *2.2 Monazite Step-Etching*

Using the 6M HCl etchant at 90°C, a step-etch experiment was carried out to determine the optimal time needed to reveal fission tracks. Twenty monazite crystals were hand-picked under a stereo microscope and annealed at 400°C for 18 hours in a block heater furnace to remove all fossil fission tracks. Crystals were then mounted in cold-setting *Epofix* epoxy on their {100} faces, slightly ground and polished, then irradiated with collimated fission fragments from a $^{252}$Cf source for 7 hours to implant a density of ~5 x $10^6$ tracks/cm$^3$. Implanted $^{252}$Cf semi-tracks (Figure 3) were used throughout this study as the track density could be easily controlled. $^{252}$Cf fission fragments have a similar mass distribution to those of $^{238}$U and therefore serve as a useful proxy for the etching of fossil tracks (Wagner and Van den haute, 1992). The implanted tracks were oriented at approximately 30° to the surface and the mount was step-etched in 15-minute increments. Imagery of each monazite grain was captured in transmitted and reflected light using a 100x dry objective on a *Zeiss* Axio Imager M1m motorised microscope fitted with a *PI* piezo-motor scanning stage and a 4 Megapixel IDS µEye USB 3 CMOS digital camera, interfaced to a control PC using *TrackWorks* software (Gleadow *et al.,* 2009). Each etching step was followed by image capture on the same grains and this was repeated until the tracks were over-etched, after a total of 90 minutes. The track densities were then determined from the captured image stacks using *FastTracks* software (Gleadow *et al.,* 2009) as shown in Figure 4 suggesting an optimum etching time of ~75 min for this sample.

--------------------------------------Figure 3 hereabouts--------------------------------------

------------------------------------ Figure 4 hereabouts ------------------------------------

### *2.3 Isothermal Annealing Analysis*

Because monazite is thought to have a relatively low annealing temperature compared to apatite, it is important to determine whether any fission-track annealing occurs during etching at 90°C (Ure, 2010; Weise *et al.,* 2009). Therefore, an isothermal annealing experiment was carried out to evaluate the degree of annealing at 90°C under laboratory timescales. About 80 pre-annealed monazite grains were manually oriented on their {100} face on double-sided tape in a control and each of five sample mounts. The samples were then mounted in cold-setting *Epofix* epoxy, slightly ground and polished, and exposed to the $^{252}Cf$ source as described in Section 2.2. After implantation, grains were removed from the epoxy mount using a commercial paint-stripper. The loose grains were then annealed in aluminium tubes in a *Ratek Digital* Dry Block Heater at 90°C for times of 1, 3, 7, 15 and 31 hours. Each aliquot was removed and quenched, then remounted by placing the grains polished-face down on double-sided tape before re-embedding in epoxy. The original polished surfaces were then etched in 6M HCl at 90°C for 1 hour. Although each sample experienced an additional hour of exposure to this temperature during etching, it is argued below that the effective etching time is very much less. Image capture was performed as for Section 2.2, and semi-track lengths determined on 500 tracks in each mount are presented in Table 1 and Figure 5.

------------------------------------- Figure 5 hereabouts ------------------------------------

***2.4 Electron Microprobe Analysis***

Both the step-etch and isothermal annealing experiments showed that the etching rate between individual monazite grains was not constant, with clear variation in the degree of etching being evident within and between grains. Electron microprobe (EMP) analyses were carried out to characterise the Harcourt monazites and evaluate possible links between elemental composition and etching rate.

Properly etched fission tracks were judged to be ~1-2 μm in width, under-etched tracks noticeably fainter and thinner, and those over-etched noticeably wider. EMP results for all sample mounts are presented in Table 2, whereas analyses for monazite grains identified as under-etched, well-etched and over-etched, are presented in Tables 3-5, respectively.

***3. Discussion***

Using the 6M HCl etchant at 90°C, step-etching (Figure 4) shows that fission tracks on monazite {100} surfaces are progressively revealed in a similar way to that observed in other minerals. Up to about 15 minutes, no tracks are visible but by ~30 minutes the track density increases rapidly, until a quasi-plateau is reached at ~60 minutes. We therefore conclude that 60 minutes is a reasonable minimum time required to etch fission tracks in the Harcourt monazite studied. Because of differences in etching-rate on {100} faces between individual grains, however, it cannot be concluded that this etching time will be suitable for every crystal. Rather, the etching required could vary between ~60-90 minutes for these monazites. In cases of extreme variability, a multi-etch procedure may be needed, where two or more monazite mounts are prepared and each etched for a different time between 60-90 minutes. This etching procedure would be important for obtaining a representative distribution of ages where different intrasample grain populations occur, as is common practice for zircon fission track dating (e.g. Naeser *et al.,* 1987).

Etching differences between grains can be attributed to a number of factors including anisotropic etching in different crystallographic orientations, elemental composition (see section 2.4) or accumulated radiation damage. It is well-known in minerals such as zircon and titanite (e.g. Gleadow, 1978; Gleadow *et al.,* 1976) that accumulated alpha-recoil damage causes fission tracks to etch more rapidly and more isotropically. Although monazite must receive a large dose of radiation damage from U and Th alpha-decay, it has never been reported in a metamict state, suggesting that it shares the same damage self-repair mechanism observed in apatite (e.g. Weise *et al.,* 2009). It is also known in other minerals (e.g. titanite) that accumulated alpha-recoil damage anneals at lower temperatures than required for fission-track annealing (Gleadow, 1978). Assuming a similar annealing relationship in monazite, with its postulated low thermal stability for fission tracks (perhaps ~50°C, Weise *et al.,* 2009), suggests that alpha-recoil damage would not be stable at ambient surface temperatures over geological time. As grains in this study have been pre-annealed to remove fossil tracks, at least some of this accumulated radiation damage is also assumed to have been removed. However, the exceptionally high abundance of U and Th (~0.40 - 7 wt. %) in monazite suggests that some radiation damage will still be present.

Figure 5 shows that significant laboratory annealing of fission-tracks in monazite occurs at 90°C with mean semi-track lengths reducing rapidly before reaching a plateau at about 80% of that of the control after 15 hours. Although at first sight this experiment suggests that track shortening of ~4% might result from etching for one hour at 90°C, the actual effect is likely to be much less. The earliest track etching experiments (Price & Walker, 1962) demonstrated that etchants penetrate almost instantaneously along the highly-reactive core of the latent track. Their TEM observations showed that in various micas, a 20% HF etchant produced well-defined hollow channels in <1 second. Subsequent enlargement of these initially ~10 nm diameter tracks to optically visible dimensions (~1 µm) occurs by dissolving the undamaged side walls of the tracks over their full etchable range, resulting in the almost parallel-sided forms typical of etched tracks in minerals, including monazite. These observations imply that the time for removing the damaged cores of the latent tracks is about three orders of magnitude less than that required to enlarge them sufficiently for optical microscopy. Assuming a similar relationship for monazite implies that the actual exposure of the annealable latent tracks to 90°C temperatures during etching is probably negligible, and certainly very much less than the ~4% shortening that would result if the tracks had been annealed over the entire duration of etching.

Ideally it would be desirable to find an etchant for monazite that could be used at a lower temperature, but our experiments failed to identify any satisfactory alternative. Simply lowering the temperature for a particular etchant and compensating with longer etching times, may not make any significant difference, as noted by Weise *et al.,* 2009, because the rate laws governing fission-track etching and annealing are probably similar.

Approximately half the major elements in Harcourt Granodiorite monazite-(Ce) were higher in Si, Y, Sm, Gd, Th and U content (particularly the last two elements) in the over-etched grains compared to under-etched and well-etched grains (see Tables 3 - 5). However, no significant chemical differences were observed between under-etched and well-etched grains. Taken at face value, we conclude, with Fayon (2011), that higher U and Th concentrations in monazite influence the etching-rate, probably due to residual radiation damage that was not removed by pre-annealing at 400°C.

***4. Conclusions***

Etching experiments on polished {100} faces in a set of monazite-(Ce) grains showed optimal results for fission track revelation using a 6M HCl etchant at 90°C for 60-90 minutes. Fission tracks produced were of excellent shape and the weaker etchant relative to previous work reduced grain corrosion and loss. Differences in etching-rate between individual grains, suggests the likely influence of composition and radiation damage. In extreme cases it may be necessary to prepare more than one mount, so that different etching times can be used to account for the range of possible fission-track age components.

Isothermal annealing experiments at 90°C showed clear evidence of fission-track annealing over times of 1 - 31 hours, confirming that monazite has a greater sensitivity to thermal annealing than apatite. Track length reductions of ~4% for one hour were observed, up to a maximum of ~20% for 15 hours or more. However, it is concluded that etching at this temperature is highly unlikely to have any measurable effect on track lengths due to the very short time (probably seconds) taken for the etchant to penetrate along the full etchable track range.

There is evidence for some compositional control (principally by U and Th) on track-etching rate between different monazite grains, further suggesting some control by accumulated radiation damage. Needle-shaped track shapes in different directions suggest that etching is dominantly isotropic, although further investigation, including experiments to address the extent of possible anisotropic etching behaviour, are required to fully understand monazite fission-track etching properties.

***Acknowledgments***

We thank Abaz Alimanovic for helpful conversations and for sourcing the different etching chemicals. Graham Hutchinson for electron microprobe analyses. The University of Melbourne thermochronology laboratory receives support under the National Collaborative Research Infrastructure Strategy AuScope program. SJ also acknowledges funding from; the Australian Government for an Australian Postgraduate Award (APA) and Melbourne University for a Baragwanath Trust Scholarship and Science Abroad Travel Scholarship (SATS). We are grateful to Cornelia Spiegel, Ewald Hejl and two other reviewers for their constructive comments and suggestions on an earlier draft of this work.

***References***

Clemens, J. D. (2018). Granitic magmas with I-type affinities , from mainly metasedimentary sources : the Harcourt batholith of southeastern Australia. *Contributions to Mineralogy and Petrology*, *173*(11), 1–20. https://doi.org/10.1007/s00410-018-1520-z

Cottle, J. M., Searle, M. P., Horstwood, M. S. A., & Waters, D. J. (2009). Timing of Midcrustal Metamorphism , Melting , and Deformation in the Mount Everest Region of Southern Tibet Revealed by U(-Th)-Pb Geochronology. *The Journal of Geology*, *117*, 643–664. https://doi.org/10.1086/605994

Erickson, T. M., Pearce, M. A., Taylor, R. J. M., Timms, N. E., Clark, C., Reddy, S. M., & Buick, I. S. (2015). Deformed monazite yields high-temperature tectonic ages. *Geology*, *43*(5), 383–386. https://doi.org/10.1130/G36533.1

Fayon, A. K. (2011). Fission Track Dating of Monazite: Etching Efficiencies as a Function of U Content. In *GSA Annual Meeting* (p. 331). Minneapolis: Geological Society of America.

Fleischer, R. L., Price, P. B., & Walker, R. M. (1975). *Nuclear Tracks in Solids*. Berkeley: University of California Press.

Gleadow, A. J. W. (1978). Anisotropic and Variable Track Etching Characteristics in Natural Sphenes. *Nuclear Track Detection*, *2*, 105–117.

Gleadow, A. J. W., Hurford, A. J., & Quaife, R. D. (1976). Fission Track Dating of Zircon: Improved Etching Techniques. *Earth*, *33*, 273–276.

Gleadow, A. J. W., Belton, D. X., Kohn, B. P., & Brown, R. W. (2002). Fission Track Dating of Phosphate Minerals and the Thermochronology of Apatite. *Reviews in Mineralogy and Geochemistry*, *48*(1), 579–630. https://doi.org/10.2138/rmg.2002.48.16

Gleadow, A. J. . W., Raza, A., Kohn, B. P., & Spencer, S. A. S. (2004). The potential of monazite as a new low-temperature fission-track thermochronomter. Amsterdam: FT2004 10th International Conference on Fission Track Dating.

Gleadow, A. J. W., Raza, A., Kohn, B. P., & Spencer, S. A. (2005). The potential of Monazite for fission-track dating. In *Accessory Mineral Geochemistry II in Goldschmidt Conference Abstracts* (p. A21). Moscow, Idaho, USA.

Gleadow, A. J. W., Gleadow, S. J., Frei, S., Kohlmann, F., & Kohn, B. P. (2009). Automated analytical techniques for fission track thermochronology. *Geochimica et Cosmochimica Acta Supplement*, *73*, A441.

Kohn, B. P., Chung, L., & Gleadow, A. J. W. (2019). Fission-Track Analysis: Field Collection, Sample Preparation and Data Acquisition. In M. G. Malusà & P. G. Fitzgerald (Eds.), *Fission-Track Thermochronology and its Application to Geology* (pp. 25–48). Springer

Textbooks in Earth Sciences, Geography and Environment. https://doi.org/https://doi.org/10.1007/978-3-319-89421-8

Naeser, N. D., Zeitler, P. K., Naeser, C. W., & Cerveny, P. F. (1987). Provenance Studies By Fission-Track Dating of Zircon -- Etching And Counting Procedures. *Nuclear Tracks and Radiation Measurements*, *13*, 121–126.

Nesse, W. D. (2012). *Introduction to Mineralogy* (2nd ed.). New York: Oxford University Press.

Peterman, E. M., Hourigan, J. K., & Grove, M. (2014). Experimental and geologic evaluation of monazite (U-Th)/He thermochronometry: Catnip Sill, Catalina Core Complex, Tucson, AZ. *Earth and Planetary Science Letters*, *403*(October 2014), 48–55. https://doi.org/10.1016/j.epsl.2014.06.020

Price, P. B., & Walker, R. M. (1962). Chemical etching of charged-particle tracks in solids. *Journal of Applied Physics*, *33*(12), 3407–3412. https://doi.org/10.1063/1.1702421

Prior, D. J., Boyle, A. P., Brenker, F., Chedadle, M. C., Day, A., Lopez, G., … Zetterström, L. (1999). The application of electron backscatter diffraction and orientation contrast imaging in the SEM to textural problems in rocks. *American Mineralogist*, *84*, 1741–1759. https://doi.org/10.2138/am-1999-11-1204

Shipley, N. K., & Fayon, A. K. (2006). Vanishing Act: Experiments on Fission Track Annealing in Monazite. In *AGU Fall Meeting Abstracts*.

Shukoljukov, J. A., & Komarov, A. N. (1970). Tracks of uranium fission in monazite (in Russian). In *Bulletin of the Commission for the Determination of the Absolute Age of Geological Formations* (pp. 20–26). Moscow: Akad. Nauk. USSR.

Ure, A. (2010). *Annealing characteristics of fission tracks in monazite: Application of a new method for performing thermal annealing experiments using implanted Cf-252 fission fragment semi-tracks. BSc (Hons) thesis, The University of Melbourne*.

Wagner, G. A., & Van den Haute, P. (1992). *Fission-Track Dating* (2nd ed.). Stuttgart: Solid Earth Sciences Library Vol.6, Kluwer Academic Publishers.

Weise, C., van den Boogaart, K. G., Jonckheere, R., & Ratschbacher, L. (2009). Annealing kinetics of Kr-tracks in monazite: Implications for fission-track modelling. *Chemical Geology*, *260*(1–2), 129–137. https://doi.org/10.1016/j.chemgeo.2008.12.014

## *Figure Captions*

**Figure 1.** a) Unetched monazite grain from the Harcourt Granodiorite. b) Corrosion of the same grain following a 60 min etch in 12 M HCl at 50°C. Arrows highlight areas where the grain has been completely lost along with the appearance of polishing scratches, together with a change in overall appearance with increased internal reflections. Both images in reflected light.

**Figure 2.** a) Typical monazite crystal morphology illustrating common crystallographic planes and axes (after mindat.org) and showing that such grains are most likely to settle on their {100} faces. b) Equal area stereographic projections from EBSD analyses of 33 grains of Harcourt monazite that were not specifically oriented during the mounting process. Each point represents the average estimate for the pole to the {100} face for a particular grain. The strong clustering shows that 26 of the 33 grains have naturally settled onto their {100} faces during mounting in epoxy resin.

**Figure 3.** a) Shows well-etched implanted $^{252}$Cf semi-tracks dipping at ~30° to the surface in a previously annealed grain of monazite from the Harcourt Granodiorite. The tracks have been implanted under vacuum and are collimated by a distance of ~2 cm from the small-area $^{252}$Cf source. For comparison b) shows the appearance of well-etched spontaneous fission-tracks from the Harcourt monazite etched in 6M HCl at 90°C for 60 min. c) Diagram showing the experimental apparatus used for exposing polished mounts to the $^{252}$Cf source. The mount carrier is enclosed within a small (10 cm diameter) acrylic chamber evacuated using a rotary pump (external radiation shielding not shown). The mount is attached to a rotatable sample holder to control the dip of the collimated semi-tracks to the surface ($l_t$ = true semi-track length).

**Figure 4.** Step-etch results of 20 Harcourt Granodiorite monazite crystals, based on a total of 15,178 $^{252}$Cf semi-tracks counted after 15 minute increments up to a total 90 minutes of etching in 6M HCl at 90°C. Diagram shows the observed increase in track density with increasing etching time. Tracks first become visible by ~15 minutes after which the track density increases rapidly to a quasi-plateau at ~60 minutes after which there is little change other than a continued increase in size of the etch-pits.

**Figure 5.** Semi-track lengths from the Harcourt monazite 90°C isothermal annealing experiment over annealing times from 1 to 31 hours. Five hundred semi-track lengths were measured over multiple grains for each annealing step, and results show the mean semi-track length corrected for dip and refractive index. The true semi-track length represents approximately half the length of an equivalent confined fission track (Ure, 2010). The average $^{252}$Cf semi-track length decreases from 4.96 μm for the unannealed control sample, to 3.99 μm after 31 hours annealing (left axis). The right axis shows the semi-track length reduction (%), normalized to the mean length of the unannealed control sample.

**Table 1.** Isothermal laboratory annealing data for $^{252}Cf$ semi-tracks in Harcourt Granodiorite monazite. The annealing time, average true semi-track length (±1σ error), track length reduction normalized to the mean length in the unannealed control sample (±1σ error), and number of tracks measured is shown for each sample mount. The annealing temperature for all samples was 90°C.

| Sample | Annealing Time (Hours) | Average Semi-Track Length (μm) | $l/l_0$ | Number of Tracks |
|---|---|---|---|---|
| ETCH-21 (Control) | 0 | 4.96 ± 0.03 | 1.00 | 500 |
| ETCH-22 | 1 | 4.76 ± 0.04 | 0.96 ± 0.010 | 500 |
| ETCH-23 | 3 | 4.55 ± 0.04 | 0.92 ± 0.010 | 500 |
| ETCH-24 | 7 | 4.33 ± 0.04 | 0.87 ± 0.010 | 500 |
| ETCH-25 | 15 | 4.00 ± 0.04 | 0.81 ± 0.009 | 500 |
| ETCH-26 | 31 | 3.99 ± 0.04 | 0.80 ± 0.009 | 500 |

**Table 2.** Average composition of Harcourt Granodiorite monazite, irrespective of etching category (±2σ error) from a total of 81 EPMA analyses (with 12 standards included in the run). Ce is the dominant REE, followed by La, Nd and Sm. $ThO_2$ and $UO_2$ show averages of 6.31 wt.% and 0.50 wt.%, respectively. Measurements made with a Cameca SX50 electron microprobe using a 10 μm beam width, 50 KeV beam current, 25 KV accelerating voltage and take off angle of 40°.

| | $SiO_2$ | $P_2O_5$ | CaO | $Y_2O_3$ | $La_2O_3$ | $Ce_2O_3$ | $Pr_2O_3$ | $Nd_2O_3$ | $Sm_2O_3$ | $Gd_2O_3$ | $ThO_2$ | $UO_2$ | Sum Ox% |
|---|---|---|---|---|---|---|---|---|---|---|---|---|---|
| **Mean** | 1.63 ± 0.04 | 27.37 ± 0.15 | 0.45 ± 0.02 | 2.39 ± 0.05 | 14.13 ± 0.17 | 28.54 ± 0.26 | 4.45 ± 0.11 | 10.61 ± 0.13 | 1.80 ± 0.08 | 1.34 ± 0.08 | 6.31 ± 0.11 | 0.50 ± 0.04 | 99.52 |

**Table 3.** Elemental compositions (±2σ) of under-etched monazite grains observed in ETCH-21, ETCH-23 and ETCH-24 sample mounts from Experiment 2. Run conditions are identical to those listed in Table 2. The average across all 26 grains shows that Ce is the dominant REE, followed by Nd > La > Sm. $ThO_2$ content averages 5.74 wt.% and $UO_2$ content averages 0.49 wt.%.

| **ETCH-21** | | | | | | | | | | | | | |
|---|---|---|---|---|---|---|---|---|---|---|---|---|---|
| **Grain Number** | **$SiO_2$** | **$P_2O_5$** | **CaO** | **$Y_2O_3$** | **$La_2O_3$** | **$Ce_2O_3$** | **$Pr_2O_3$** | **$Nd_2O_3$** | **$Sm_2O_3$** | **$Gd_2O_3$** | **$ThO_2$** | **$UO_2$** | **Sum Oxide%** |
| Grain 01 | 1.19 ± 0.04 | 27.58 ± 0.15 | 0.42 ± 0.02 | 3.85 ± 0.06 | 13.38 ± 0.16 | 27.92 ± 0.26 | 4.37 ± 0.11 | 11.00 ± 0.13 | 2.02 ± 0.08 | 1.61 ± 0.08 | 4.67 ± 0.10 | 0.50 ± 0.04 | 98.51 |
| Grain 15 | 1.02 ± 0.04 | 28.11 ± 0.15 | 0.38 ± 0.02 | 2.36 ± 0.05 | 15.33 ± 0.18 | 30.37 ± 0.27 | 4.66 ± 0.11 | 10.50 ± 0.13 | 1.76 ± 0.08 | 1.37 ± 0.07 | 3.45 ± 0.09 | 0.37 ± 0.04 | 99.68 |
| Grain 29 | 0.70 ± 0.04 | 28.86 ± 0.16 | 0.40 ± 0.02 | 3.22 ± 0.06 | 14.40 ± 0.17 | 29.88 ± 0.27 | 4.65 ± 0.11 | 11.07 ± 0.13 | 1.97 ± 0.08 | 1.47 ± 0.08 | 2.39 ± 0.08 | 0.54 ± 0.04 | 99.56 |
| Grain 31 | 1.73 ± 0.04 | 26.75 ± 0.15 | 0.42 ± 0.02 | 2.37 ± 0.05 | 14.10 ± 0.17 | 28.09 ± 0.26 | 4.48 ± 0.11 | 10.58 ± 0.13 | 1.89 ± 0.08 | 1.42 ± 0.08 | 6.10 ± 0.11 | 0.44 ± 0.04 | 98.38 |
| Grain 32 | 1.38 ± 0.4 | 28.29 ± 0.15 | 0.39 ± 0.02 | 1.99 ± 0.05 | 15.26 ± 0.18 | 29.59 ± 0.27 | 4.49 ± 0.11 | 10.86 ± 0.13 | 1.74 ± 0.08 | 1.26 ± 0.07 | 4.71 ± 0.10 | 0.37 ± 0.04 | 100.35 |
| Grain 36 | 1.36 ± 0.04 | 27.93 ± 0.15 | 0.35 ± 0.02 | 2.52 ± 0.05 | 15.59 ± 0.18 | 29.82 ± 0.27 | 4.51 ± 0.11 | 10.29 ± 0.13 | 1.62 ± 0.08 | 1.17 ± 0.07 | 4.42 ± 0.09 | 0.53 ± 0.04 | 100.12 |
| Grain 43 | 1.13 ± 0.04 | 28.74 ± 0.16 | 0.43 ± 0.02 | 2.55 ± 0.05 | 14.78 ± 0.17 | 29.68 ± 0.27 | 4.54 ± 0.11 | 10.68 ± 0.13 | 1.89 ± 0.08 | 1.40 ± 0.08 | 4.21 ± 0.09 | 0.43 ± 0.04 | 100.45 |
| Grain 56 | 1.24 ± 0.04 | 28.92 ± 0.16 | 0.38 ± 0.02 | 2.81 ± 0.06 | 14.92 ± 0.17 | 29.47 ± 0.27 | 4.40 ± 0.11 | 10.46 ± 0.13 | 1.79 ± 0.08 | 1.41 ± 0.08 | 4.17 ± 0.09 | 0.43 ± 0.04 | 100.40 |
| Grain 59 | 1.03 ± 0.04 | 29.04 ± 0.16 | 0.42 ± 0.02 | 2.14 ± 0.05 | 15.72 ± 0.18 | 30.71 ± 0.28 | 4.47 ± 0.11 | 10.52 ± 0.13 | 1.62 ± 0.08 | 1.15 ± 0.07 | 3.43 ± 0.09 | 0.38 ± 0.04 | 100.63 |
| Grain 70 | 2.01 ± 0.04 | 27.21 ± 0.15 | 0.46 ± 0.02 | 2.71 ± 0.05 | 14.07 ± 0.17 | 27.86 ± 0.26 | 4.23 ± 0.11 | 10.27 ± 0.13 | 1.76 ± 0.08 | 1.30 ± 0.08 | 6.37 ± 0.11 | 0.61 ± 0.04 | 98.88 |
| **ETCH-23** | | | | | | | | | | | | | |
| Grain 09 | 1.25 ± 0.04 | 28.03 ± 0.15 | 0.40 ± 0.02 | 2.79 ± 0.06 | 13.55 ± 0.16 | 28.71 ± 0.26 | 4.57 ± 0.11 | 11.55 ± 0.14 | 2.06 ± 0.08 | 1.56 ± 0.08 | 4.50 ± 0.10 | 0.43 ± 0.04 | 99.39 |
| Grain 12 | 1.86 ± 0.04 | 27.36 ± 0.15 | 0.43 ± 0.02 | 2.75 ± 0.06 | 13.72 ± 0.16 | 28.32 ± 0.26 | 4.38 ± 0.11 | 10.87 ± 0.13 | 1.96 ± 0.08 | 1.51 ± 0.08 | 6.47 ± 0.11 | 0.74 ± 0.04 | 100.38 |
| Grain 30 | 1.08 ± 0.04 | 28.27 ± 0.15 | 0.42 ± 0.02 | 1.75 ± 0.05 | 15.59 ± 0.18 | 30.48 ± 0.28 | 4.70 ± 0.11 | 10.61 ± 0.13 | 1.69 ± 0.08 | 1.12 ± 0.07 | 4.08 ± 0.09 | 0.32 ± 0.04 | 100.11 |
| Grain 42 | 2.04 ± 0.04 | 26.86 ± 0.15 | 0.47 ± 0.02 | 2.29 ± 0.05 | 13.19 ± 0.16 | 27.53 ± 0.25 | 4.40 ± 0.11 | 10.73 ± 0.13 | 1.86 ± 0.08 | 1.36 ± 0.08 | 8.88 ± 0.12 | 0.52 ± 0.04 | 100.14 |
| Grain 54 | 0.83 ± 0.04 | 29.38 ± 0.`16 | 0.35 ± 0.02 | 1.53 ± 0.05 | 15.51 ± 0.18 | 31.36 ± 0.28 | 4.59 ± 0.11 | 10.76 ± 0.13 | 1.45 ± 0.08 | 0.96 ± 0.07 | 3.77 ± 0.09 | 0.28 ± 0.04 | 100.77 |
| Grain 62 | 1.54 ± 0.04 | 28.23 ± 0.15 | 0.54 ± 0.02 | 1.58 ± 0.05 | 15.25 ± 0.18 | 29.68 ± 0.27 | 4.50 ± 0.11 | 10.47 ± 0.13 | 1.66 ± 0.08 | 1.18 ± 0.07 | 5.19 ± 0.10 | 0.53 ± 0.04 | 100.34 |
| **ETCH-24** | | | | | | | | | | | | | |
| Grain 08 | 1.42 ± 0.04 | 27.39 ± 0.15 | 0.43 ± 0.02 | 2.66 ± 0.05 | 14.20 ± 0.17 | 28.56 ± 0.26 | 4.50 ± 0.11 | 10.50 ± 0.13 | 1.86 ± 0.08 | 1.39 ± 0.08 | 5.57 ± 0.10 | 0.56 ± 0.04 | 99.06 |
| Grain 09 | 1.59 ± 0.04 | 27.13 ± 0.15 | 0.50 ± 0.02 | 1.39 ± 0.05 | 15.22 ± 0.18 | 29.18 ± 0.26 | 4.69 ± 0.11 | 10.13 ± 0.12 | 1.49 ± 0.08 | 0.98 ± 0.07 | 6.60 ± 0.11 | 0.35 ± 0.04 | 99.25 |
| Grain 16 | 1.67 ± 0.04 | 26.52 ± 0.15 | 0.40 ± 0.02 | 2.51 ± 0.05 | 14.02 ± 0.17 | 28.20 ± 0.26 | 4.54 ± 0.11 | 10.32 ± 0.13 | 1.85 ± 0.08 | 1.40 ± 0.08 | 6.21 ± 0.11 | 0.59 ± 0.04 | 98.24 |

| | | | | | | | | | | | | |
|---|---|---|---|---|---|---|---|---|---|---|---|---|
| Grain 23 | 1.09 ± 0.04 | 27.43 ± 0.15 | 0.40 ± 0.02 | 2.39 ± 0.05 | 15.67 ± 0.18 | 30.97 ± 0.28 | 4.73 ± 0.11 | 10.16 ± 0.12 | 1.33 ± 0.08 | 0.84 ± 0.07 | 2.84 ± 0.08 | 0.89 ± 0.04 | 98.74 |
| Grain 25 | 0.92 ± 0.04 | 27.44 ± 0.15 | 0.41 ± 0.02 | 2.50 ± 0.05 | 14.80 ± 0.17 | 30.02 ± 0.27 | 4.74 ± 0.11 | 10.51 ± 0.13 | 1.77 ± 0.08 | 1.46 ± 0.08 | 3.18 ± 0.09 | 0.38 ± 0.04 | 98.13 |
| Grain 32 | 1.43 ± 0.04 | 27.38 ± 0.15 | 0.38 ± 0.02 | 1.96 ± 0.05 | 14.88 ± 0.17 | 29.74 ± 0.27 | 4.64 ± 0.11 | 10.53 ± 0.13 | 1.71 ± 0.08 | 1.22 ± 0.07 | 5.53 ± 0.10 | 0.41 ± 0.04 | 99.80 |
| Grain 44 | 1.16 ± 0.04 | 28.26 ± 0.15 | 0.42 ± 0.02 | 2.16 ± 0.05 | 14.57 ± 0.17 | 30.27 ± 0.27 | 4.69 ± 0.11 | 11.03 ± 0.13 | 1.82 ± 0.08 | 1.35 ± 0.07 | 3.89 ± 0.09 | 0.40 ± 0.04 | 100.01 |
| Grain 50 | 0.51 ± 0.03 | 29.05 ± 0.16 | 0.95 ± 0.02 | 2.25 ± 0.05 | 13.49 ± 0.16 | 28.23 ± 0.26 | 4.44 ± 0.11 | 11.46 ± 0.13 | 2.15 ± 0.08 | 1.62 ± 0.08 | 5.23 ± 0.10 | 0.22 ± 0.04 | 99.59 |
| Grain 80 | 4.81 ± 0.06 | 22.62 ± 0.13 | 0.47 ± 0.02 | 1.83 ± 0.05 | 10.33 ± 0.14 | 22.92 ± 0.22 | 3.73 ± 0.10 | 10.40 ± 0.13 | 1.85 ± 0.08 | 1.35 ± 0.08 | 19.27 ± 0.18 | 0.80 ± 0.04 | 100.37 |
| Grain 83 | 3.06 ± 0.05 | 24.9 ± 0.14 | 0.58 ± 0.02 | 2.76 ± 0.05 | 10.38 ± 0.14 | 24.09 ± 0.23 | 3.94 ± 0.10 | 11.29 ± 0.13 | 2.18 ± 0.08 | 1.63 ± 0.08 | 14.09 ± 0.15 | 0.65 ± 0.04 | 99.54 |
| **Mean** | **1.50 ± 0.04** | **27.60 ± 0.15** | **0.45 ± 0.02** | **2.37 ± 0.05** | **10.38 ± 0.17** | **28.91 ± 0.26** | **4.48 ± 0.11** | **10.68 ± 0.13** | **1.80 ± 0.08** | **1.33 ± 0.08** | **5.74 ± 0.10** | **0.49 ± 0.04** | **99.65** |

**Table 4.** Elemental compositions (±2σ) of well-etched monazite grains observed in ETCH-21, ETCH-23 and ETCH-24 sample mounts from Experiment 2. Run conditions are identical to those listed in Table 2. As for the under-etched set of crystals, this set also indicates Ce as the dominant REE, followed by La, Nd and Sm (29 analyses). $ThO_2$ and $UO_2$ average 5.60 wt.% and 0.46 wt.%, respectively.

| **ETCH-21** | | | | | | | | | | | | | |
|---|---|---|---|---|---|---|---|---|---|---|---|---|---|
| **Grain Number** | **$SiO_2$** | **$P_2O_5$** | **CaO** | **$Y_2O_3$** | **$La_2O_3$** | **$Ce_2O_3$** | **$Pr_2O_3$** | **$Nd_2O_3$** | **$Sm_2O_3$** | **$Gd_2O_3$** | **$ThO_2$** | **$UO_2$** | **Sum Oxide %** |
| Grain 02 | 1.72 ± 0.04 | 27.38 ± 0.15 | 0.42 ± 0.02 | 2.49 ± 0.05 | 14.66 ± 0.17 | 28.75 ± 0.26 | 4.38 ± 0.11 | 10.55 ± 0.13 | 1.87 ± 0.08 | 1.35 ± 0.08 | 5.32 ± 0.10 | 0.59 ± 0.04 | 99.46 |
| Grain 03 | 1.65 ± 0.04 | 26.66 ± 0.15 | 0.47 ± 0.02 | 2.47 ± 0.05 | 14.63 ± 0.17 | 28.52 ± 0.26 | 4.53 ± 0.11 | 10.24 ± 0.13 | 1.76 ± 0.08 | 1.34 ± 0.08 | 6.05 ± 0.11 | 0.57 ± 0.04 | 98.90 |
| Grain 04 | 1.59 ± 0.04 | 27.02 ± 0.15 | 0.43 ± 0.02 | 2.58 ± 0.05 | 14.76 ± 0.17 | 28.80 ± 0.26 | 4.48 ± 0.11 | 10.25 ± 0.12 | 1.77 ± 0.08 | 1.26 ± 0.07 | 5.36 ± 0.10 | 0.64 ± 0.04 | 98.94 |
| Grain 08 | 1.66 ± 0.04 | 27.09 ± 0.15 | 0.40 ± 0.02 | 2.61 ± 0.05 | 14.57 ± 0.17 | 29.01 ± 0.26 | 4.47 ± 0.11 | 10.31 ± 0.13 | 1.81 ± 0.08 | 1.32 ± 0.08 | 5.64 ± 0.10 | 0.55 ± 0.04 | 99.43 |
| Grain 10 | 2.36 ± 0.04 | 26.40 ± 0.15 | 0.45 ± 0.02 | 2.08 ± 0.05 | 13.71 ± 0.16 | 27.46 ± 0.25 | 4.29 ± 0.11 | 10.47 ± 0.13 | 1.83 ± 0.08 | 1.29 ± 0.08 | 9.02 ± 0.12 | 0.49 ± 0.04 | 99.85 |
| Grain 17 | 1.17 ± 0.04 | 27.99 ± 0.15 | 0.42 ± 0.02 | 1.36 ± 0.05 | 16.42 ± 0.19 | 30.67 ± 0.28 | 4.81 ± 0.11 | 10.14 ± 0.12 | 1.49 ± 0.08 | 0.92 ± 0.07 | 4.24 ± 0.09 | 0.28 ± 0.04 | 99.90 |
| Grain 20 | 1.37 ± 0.04 | 27.95 ± 0.15 | 0.36 ± 0.02 | 2.54 ± 0.05 | 14.55 ± 0.17 | 29.49 ± 0.27 | 4.56 ± 0.11 | 10.83 ± 0.13 | 1.81 ± 0.08 | 1.34 ± 0.08 | 4.15 ± 0.09 | 0.47 ± 0.04 | 99.41 |
| Grain 27 | 1.24 ± 0.04 | 27.59 ± 0.15 | 0.41 ± 0.02 | 2.70 ± 0.05 | 14.95 ± 0.17 | 29.84 ± 0.27 | 4.54 ± 0.11 | 10.41 ± 0.13 | 1.76 ± 0.08 | 1.27 ± 0.07 | 3.92 ± 0.09 | 0.46 ± 0.04 | 99.09 |
| Grain 28 | 1.13 ± 0.04 | 28.71 ± 0.15 | 0.43 ± 0.02 | 0.78 ± 0.05 | 16.59 ± 0.19 | 31.62 ± 0.28 | 4.87 ± 0.11 | 10.41 ± 0.13 | 1.41 ± 0.08 | 0.75 ± 0.07 | 3.96 ± 0.09 | 0.27 ± 0.04 | 100.92 |
| Grain 30 | 1.21 ± 0.04 | 28.61 ± 0.15 | 0.64 ± 0.02 | 1.05 ± 0.05 | 15.97 ± 0.18 | 30.76 ± 0.28 | 4.79 ± 0.11 | 10.34 ± 0.13 | 1.33 ± 0.08 | 0.67 ± 0.07 | 5.16 ± 0.10 | 0.31 ± 0.04 | 100.85 |
| **ETCH-23** | | | | | | | | | | | | | |
| Grain 26 | 1.77 ± 0.04 | 27.52 ± 0.15 | 0.42 ± 0.02 | 2.82 ± 0.06 | 13.88 ± 0.17 | 28.38 ± 0.26 | 4.41 ± 0.11 | 10.40 ± 0.13 | 1.89 ± 0.08 | 1.40 ± 0.08 | 6.33 ± 0.11 | 0.59 ± 0.04 | 99.81 |

| | | | | | | | | | | | | |
|---|---|---|---|---|---|---|---|---|---|---|---|---|
| Grain 27 | 1.89 ± 0.04 | 27.56 ± 0.15 | 0.47 ± 0.02 | 2.31 ± 0.05 | 14.27 ± 0.17 | 28.62 ± 0.26 | 4.42 ± 0.11 | 10.28 ± 0.13 | 1.70 ± 0.08 | 1.28 ± 0.07 | 7.18 ± 0.11 | 0.57 ± 0.04 | 100.55 |
| Grain 31 | 1.02 ± 0.04 | 29.02 ± 0.16 | 0.46 ± 0.02 | 2.56 ± 0.05 | 14.21 ± 0.17 | 29.69 ± 0.27 | 4.51 ± 0.11 | 10.87 ± 0.13 | 1.89 ± 0.08 | 1.46 ± 0.08 | 4.44 ± 0.10 | 0.47 ± 0.04 | 100.59 |
| Grain 41 | 1.96 ± 0.04 | 27.34 ± 0.15 | 0.44 ± 0.02 | 2.09 ± 0.05 | 13.77 ± 0.16 | 28.25 ± 0.26 | 4.40 ± 0.11 | 10.79 ± 0.13 | 1.83 ± 0.08 | 1.29 ± 0.07 | 7.41 ± 0.12 | 0.47 ± 0.04 | 100.03 |
| Grain 44 | 0.81 ± 0.04 | 28.99 ± 0.15 | 0.45 ± 0.02 | 1.12 ± 0.05 | 15.72 ± 0.18 | 31.56 ± 0.28 | 4.78 ± 0.11 | 10.47 ± 0.13 | 1.38 ± 0.08 | 0.86 ± 0.07 | 3.75 ± 0.09 | 0.47 ± 0.04 | 100.35 |
| Grain 48 | 0.88 ± 0.04 | 28.58 ± 0.16 | 0.36 ± 0.02 | 3.37 ± 0.06 | 15.28 ± 0.18 | 30.31 ± 0.27 | 4.58 ± 0.11 | 10.30 ± 0.13 | 1.50 ± 0.08 | 1.18 ± 0.07 | 2.49 ± 0.08 | 0.58 ± 0.04 | 99.42 |
| Grain 53 | 1.93 ± 0.04 | 27.69 ± 0.15 | 0.55 ± 0.02 | 2.85 ± 0.06 | 12.97 ± 0.17 | 26.91 ± 0.25 | 4.25 ± 0.11 | 10.84 ± 0.13 | 2.01 ± 0.08 | 1.53 ± 0.08 | 8.31 ± 0.12 | 0.64 ± 0.04 | 100.50 |
| Grain 55 | 1.43 ± 0.04 | 28.31 ± 0.15 | 0.40 ± 0.02 | 2.53 ± 0.05 | 14.72 ± 0.16 | 29.24 ± 0.27 | 4.50 ± 0.11 | 10.44 ± 0.13 | 1.79 ± 0.08 | 1.39 ± 0.08 | 4.83 ± 0.10 | 0.45 ± 0.04 | 100.03 |
| Grain 56 | 1.64 ± 0.04 | 28.28 ± 0.15 | 0.50 ± 0.02 | 1.41 ± 0.05 | 15.18 ± 0.18 | 29.63 ± 0.27 | 4.46 ± 0.11 | 10.30 ± 0.13 | 1.53 ± 0.08 | 1.08 ± 0.07 | 6.50 ± 0.11 | 0.32 ± 0.04 | 100.85 |
| Grain 59 | 1.04 ± 0.04 | 28.9 ± 0.16 | 0.33 ± 0.01 | 2.10 ± 0.05 | 16.22 ± 0.18 | 30.67 ± 0.28 | 4.72 ± 0.11 | 11.64 ± 0.12 | 1.34 ± 0.08 | 0.83 ± 0.07 | 3.26 ± 0.09 | 0.50 ± 0.04 | 100.03 |
| **ETCH-24** | | | | | | | | | | | | | |
| Grain 02 | 0.92 ± 0.04 | 28.12 ± 0.15 | 0.46 ± 0.02 | 1.00 ± 0.05 | 16.66 ± 0.19 | 30.98 ± 0.28 | 4.85 ± 0.11 | 9.98 ± 0.12 | 1.29 ± 0.07 | 0.75 ± 0.07 | 3.73 ± 0.09 | 0.25 ± 0.04 | 98.98 |
| Grain 03 | 1.75 ± 0.04 | 27.01 ± 0.15 | 0.41 ± 0.02 | 2.25 ± 0.05 | 13.18 ± 0.16 | 27.26 ± 0.25 | 4.38 ± 0.11 | 11.23 ± 0.13 | 2.07 ± 0.08 | 1.52 ± 0.08 | 7.69 ± 0.12 | 0.38 ± 0.04 | 99.13 |
| Grain 05 | 1.94 ± 0.04 | 26.29 ± 0.15 | 0.48 ± 0.02 | 1.82 ± 0.05 | 13.75 ± 0.16 | 27.80 ± 0.26 | 4.51 ± 0.11 | 10.65 ± 0.13 | 1.76 ± 0.08 | 1.30 ± 0.07 | 7.85 ± 0.12 | 0.45 ± 0.04 | 98.59 |
| Grain 06 | 1.31 ± 0.04 | 27.21 ± 0.15 | 0.46 ± 0.02 | 2.57 ± 0.05 | 14.40 ± 0.17 | 28.77 ± 0.26 | 4.50 ± 0.11 | 10.29 ± 0.12 | 1.79 ± 0.08 | 1.37 ± 0.08 | 5.56 ± 0.10 | 0.50 ± 0.04 | 98.73 |
| Grain 11 | 0.56 ± 0.04 | 28.51 ± 0.15 | 0.88 ± 0.02 | 1.54 ± 0.05 | 14.37 ± 0.17 | 28.38 ± 0.26 | 4.63 ± 0.11 | 11.66 ± 0.14 | 1.79 ± 0.08 | 1.30 ± 0.07 | 4.97 ± 0.10 | 0.20 ± 0.04 | 98.78 |
| Grain 15 | 1.44 ± 0.04 | 26.99 ± 0.15 | 0.39 ± 0.02 | 2.81 ± 0.06 | 14.16 ± 0.17 | 28.46 ± 0.26 | 4.46 ± 0.11 | 10.51 ± 0.13 | 1.79 ± 0.08 | 1.47 ± 0.08 | 5.64 ± 0.10 | 0.57 ± 0.04 | 98.70 |
| Grain 26 | 1.46 ± 0.04 | 27.39 ± 0.15 | 0.44 ± 0.02 | 2.21 ± 0.05 | 14.48 ± 0.17 | 29.44 ± 0.27 | 4.71 ± 0.11 | 10.61 ± 0.13 | 1.78 ± 0.08 | 1.36 ± 0.08 | 5.31 ± 0.10 | 0.43 ± 0.04 | 99.62 |
| Grain 27 | 1.90 ± 0.04 | 26.05 ± 0.15 | 0.47 ± 0.02 | 2.24 ± 0.05 | 13.34 ± 0.16 | 27.58 ± 0.25 | 4.46 ± 0.11 | 10.51 ± 0.13 | 1.85 ± 0.08 | 1.45 ± 0.08 | 8.69 ± 0.12 | 0.48 ± 0.04 | 99.02 |
| **Mean** | **1.46 ± 0.04** | **27.68 ± 0.15** | **0.46 ± 0.02** | **2.15 ± 0.05** | **14.69 ± 0.17** | **29.17 ± 0.27** | **4.54 ± 0.11** | **10.51 ± 0.13** | **1.71 ± 0.08** | **1.23 ± 0.08** | **5.60 ± 0.10** | **0.46 ± 0.04** | **99.66** |

**Table 5.** Elemental compositions (±2σ) of over-etched monazite grains observed in ETCH-21, ETCH-23 and ETCH-24 sample mounts from Experiment 2. Run conditions are identical to those listed in Table 2. Based on these analyses from 27 grains, 6 elements in this category (including Si, Y, Sm, Gd, Th and U) show higher concentrations than in the under-etched and well- etched categories. $ThO_2$ is noticeably higher by over 2 wt.%, averaging 7.81 wt.%. $UO_2$ with an average of 0.58 wt.%, is also noticeably higher.

| **ETCH-21** | | | | | | | | | | | | | |
|---|---|---|---|---|---|---|---|---|---|---|---|---|---|
| **Grain Number** | **$SiO_2$** | **$P_2O_5$** | **CaO** | **$Y_2O_3$** | **$La_2O_3$** | **$Ce_2O_3$** | **$Pr_2O_3$** | **$Nd_2O_3$** | **$Sm_2O_3$** | **$Gd_2O_3$** | **$ThO_2$** | **$UO_2$** | **Sum Oxide %** |
| Grain 19 | 3.43 ± 0.05 | 25.38 ± 0.14 | 0.46 ± 0.02 | 2.76 ± 0.06 | 10.70 ± 0.14 | 24.13 ± 0.23 | 3.96 ± 0.10 | 11.56 ± 0.14 | 2.31 ± 0.09 | 1.66 ± 0.08 | 12.45 ± 0.15 | 0.67 ± 0.04 | 99.46 |

| | | | | | | | | | | | | | |
|---|---|---|---|---|---|---|---|---|---|---|---|---|---|
| Grain 24 | 1.35 ± 0.04 | 27.87 ± 0.15 | 0.48 ± 0.02 | 2.83 ± 0.06 | 13.26 ± 0.16 | 27.90 ± 0.26 | 4.37 ± 0.11 | 11.21 ± 0.13 | 2.08 ± 0.08 | 1.69 ± 0.08 | 5.84 ± 0.10 | 0.44 ± 0.04 | 99.32 |
| Grain 38 | 1.83 ± 0.04 | 27.18 ± 0.15 | 0.84 ± 0.02 | 3.30 ± 0.06 | 11.57 ± 0.15 | 25.22 ± 0.24 | 4.20 ± 0.11 | 11.44 ± 0.13 | 2.20 ± 0.08 | 1.83 ± 0.08 | 9.09 ± 0.13 | 0.59 ± 0.04 | 99.29 |
| Grain 39 | 2.24 ± 0.05 | 27.28 ± 0.15 | 0.24 ± 0.01 | 1.52 ± 0.05 | 15.71 ± 0.18 | 29.60 ± 0.27 | 4.35 ± 0.11 | 9.87 ± 0.12 | 1.36 ± 0.08 | 0.81 ± 0.07 | 7.44 ± 0.12 | 0.62 ± 0.04 | 101.05 |
| Grain 44 | 2.43 ± 0.05 | 26.16 ± 0.15 | 0.33 ± 0.02 | 1.72 ± 0.05 | 14.89 ± 0.17 | 28.43 ± 0.26 | 4.39 ± 0.11 | 9.71 ± 0.12 | 1.41 ± 0.08 | 0.96 ± 0.07 | 8.40 ± 0.12 | 0.68 ± 0.04 | 99.51 |
| **ETCH-23** | | | | | | | | | | | | | |
| Grain 11 | 1.53 ± 0.04 | 27.84 ± 0.15 | 0.39 ± 0.02 | 2.47 ± 0.05 | 13.27 ± 0.16 | 28.20 ± 0.26 | 4.45 ± 0.11 | 11.38 ± 0.13 | 2.02 ± 0.08 | 1.64 ± 0.08 | 6.32 ± 0.11 | 0.50 ± 0.04 | 100.01 |
| Grain 28 | 2.24 ± 0.04 | 27.08 ± 0.15 | 0.53 ± 0.02 | 3.17 ± 0.06 | 12.18 ± 0.15 | 25.97 ± 0.24 | 4.16 ± 0.11 | 10.88 ± 0.13 | 2.08 ± 0.08 | 1.69 ± 0.08 | 9.45 ± 0.13 | 0.58 ± 0.04 | 100.02 |
| Grain 34 | 2.93 ± 0.05 | 24.44 ± 0.14 | 0.35 ± 0.02 | 1.92 ± 0.05 | 13.96 ± 0.17 | 27.15 ± 0.25 | 4.24 ± 0.11 | 9.55 ± 0.12 | 1.48 ± 0.08 | 1.03 ± 0.07 | 10.40 ± 0.13 | 0.90 ± 0.04 | 98.35 |
| Grain 51 | 1.91 ± 0.04 | 27.36 ± 0.15 | 0.45 ± 0.02 | 2.61 ± 0.05 | 14.04 ± 0.17 | 28.29 ± 0.26 | 4.34 ± 0.11 | 10.04 ± 0.12 | 1.81 ± 0.08 | 1.37 ± 0.08 | 7.32 ± 0.11 | 0.59 ± 0.04 | 100.14 |
| Grain 57 | 2.78 ± 0.05 | 25.61 ± 0.14 | 0.46 ± 0.02 | 1.76 ± 0.05 | 12.61 ± 0.16 | 25.87 ± 0.24 | 4.06 ± 0.11 | 10.88 ± 0.13 | 1.85 ± 0.08 | 1.29 ± 0.07 | 11.71 ± 0.14 | 0.49 ± 0.04 | 99.39 |
| Grain 67 | 1.48 ± 0.04 | 27.53 ± 0.15 | 0.51 ± 0.02 | 3.94 ± 0.06 | 12.66 ± 0.16 | 26.54 ± 0.25 | 4.23 ± 0.11 | 10.94 ± 0.13 | 2.15 ± 0.08 | 1.87 ± 0.08 | 6.44 ± 0.11 | 0.53 ± 0.04 | 98.82 |
| Grain 77 | 1.99 ± 0.04 | 26.14 ± 0.15 | 0.51 ± 0.02 | 3.11 ± 0.06 | 12.48 ± 0.15 | 26.24 ± 0.25 | 4.21 ± 0.11 | 10.42 ± 0.13 | 2.04 ± 0.08 | 1.68 ± 0.08 | 8.66 ± 0.12 | 0.66 ± 0.04 | 98.13 |
| Grain 78 | 2.17 ± 0.04 | 27.16 ± 0.15 | 0.45 ± 0.02 | 2.87 ± 0.06 | 12.90 ± 0.16 | 26.73 ± 0.25 | 4.21 ± 0.11 | 10.96 ± 0.13 | 2.19 ± 0.08 | 1.62 ± 0.08 | 7.45 ± 0.12 | 0.60 ± 0.04 | 99.29 |
| **ETCH-24** | | | | | | | | | | | | | |
| Grain 04 | 3.17 ± 0.05 | 24.46 ± 0.14 | 0.53 ± 0.02 | 2.00 ± 0.05 | 11.47 ± 0.15 | 24.93 ± 0.24 | 4.08 ± 0.11 | 11.13 ± 0.13 | 2.03 ± 0.08 | 1.45 ± 0.08 | 13.13 ± 0.15 | 0.55 ± 0.04 | 98.94 |
| Grain 12 | 1.36 ± 0.04 | 27.65 ± 0.15 | 0.48 ± 0.02 | 2.34 ± 0.05 | 13.82 ± 0.16 | 28.39 ± 0.26 | 4.46 ± 0.11 | 10.99 ± 0.13 | 1.86 ± 0.08 | 1.44 ± 0.08 | 5.75 ± 0.10 | 0.46 ± 0.04 | 98.99 |
| Grain 19 | 2.34 ± 0.04 | 25.44 ± 0.14 | 0.37 ± 0.02 | 2.57 ± 0.05 | 12.52 ± 0.15 | 26.61 ± 0.25 | 4.18 ± 0.11 | 10.63 ± 0.13 | 1.92 ± 0.08 | 1.54 ± 0.08 | 10.07 ± 0.13 | 0.63 ± 0.04 | 98.83 |
| Grain 20 | 0.86 ± 0.04 | 27.76 ± 0.15 | 0.41 ± 0.02 | 3.37 ± 0.06 | 14.47 ± 0.17 | 29.35 ± 0.27 | 4.63 ± 0.11 | 10.6 ± 0.13 | 1.82 ± 0.08 | 1.47 ± 0.08 | 3.35 ± 0.09 | 0.42 ± 0.04 | 98.53 |
| Grain 22 | 0.77 ± 0.04 | 27.95 ± 0.15 | 0.43 ± 0.02 | 3.50 ± 0.06 | 14.08 ± 0.17 | 29.16 ± 0.26 | 4.52 ± 0.11 | 10.72 ± 0.13 | 1.90 ± 0.08 | 1.65 ± 0.08 | 3.04 ± 0.09 | 0.43 ± 0.04 | 98.15 |
| Grain 42 | 1.83 ± 0.04 | 26.83 ± 0.15 | 0.46 ± 0.02 | 2.46 ± 0.05 | 14.51 ±0.17 | 28.73 ± 0.26 | 4.34 ± 0.11 | 9.86 ± 0.12 | 1.70 ± 0.08 | 1.29 ± 0.07 | 6.75 ± 0.11 | 0.58 ± 0.04 | 99.34 |
| Grain 47 | 1.63 ± 0.04 | 27.00 ± 0.15 | 0.45 ± 0.02 | 2.86 ± 0.06 | 13.92 ± 0.16 | 28.78 ± 0.26 | 4.42 ± 0.11 | 10.37 ± 0.13 | 1.90 ± 0.08 | 1.48 ± 0.08 | 5.98 ± 0.11 | 0.53 ± 0.04 | 99.32 |
| Grain 48 | 1.85 ± 0.04 | 26.88 ± 0.15 | 0.48 ± 0.02 | 2.72 ± 0.05 | 13.67 ± 0.16 | 28.20 ± 0.26 | 4.39 ± 0.11 | 10.60 ± 0.13 | 1.86 ± 0.08 | 1.34 ± 0.08 | 6.70 ± 0.11 | 0.62 ± 0.04 | 99.32 |
| Grain 55 | 1.61 ± 0.04 | 27.36 ± 0.15 | 0.43 ± 0.02 | 2.25 ± 0.05 | 14.61 ± 0.17 | 28.75 ± 0.26 | 4.52 ± 0.11 | 10.54 ± 0.13 | 1.85 ± 0.08 | 1.41 ± 0.07 | 5.93 ± 0.10 | 0.49 ± 0.04 | 99.75 |
| Grain 63 | 1.72 ± 0.04 | 26.47 ± 0.15 | 0.51 ± 0.02 | 4.37 ± 0.06 | 11.71 ± 0.15 | 25.64 ± 0.24 | 4.06 ± 0.11 | 10.82 ± 0.13 | 2.21 ± 0.08 | 1.94 ± 0.08 | 8.03 ± 0.12 | 0.68 ± 0.04 | 98.15 |
| **Mean** | **1.98 ± 0.04** | **26.73 ± 0.15** | **0.46 ± 0.02** | **2.71 ± 0.05** | **13.26 ± 0.16** | **27.34 ± 0.25** | **4.29 ± 0.11** | **10.66 ± 0.13** | **1.91 ± 0.08** | **1.48 ± 0.08** | **7.81 ± 0.12** | **0.58 ± 0.04** | **99.22** |

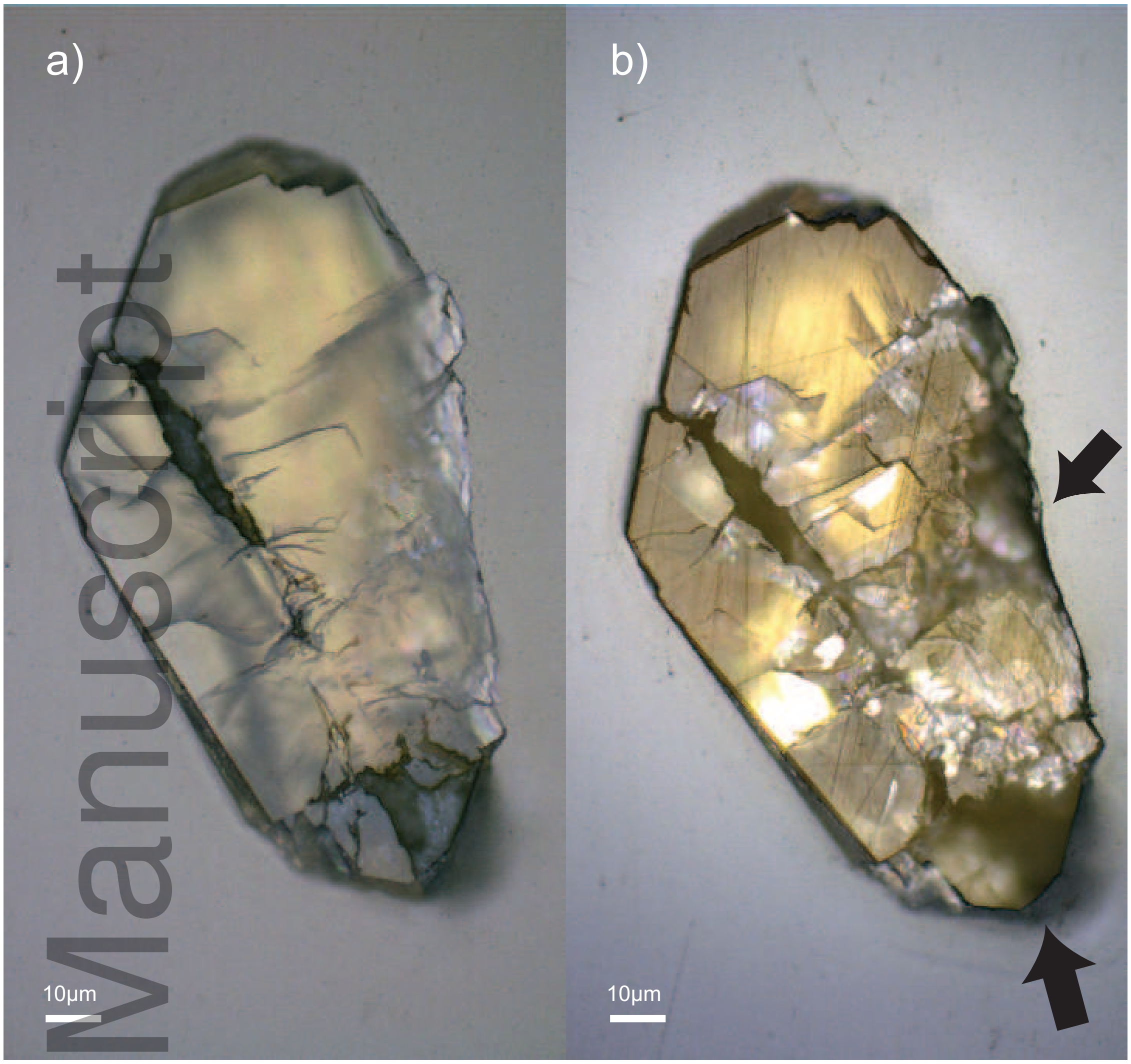




ter_12382_f1.eps

ter_12382_f2.eps

a) b)

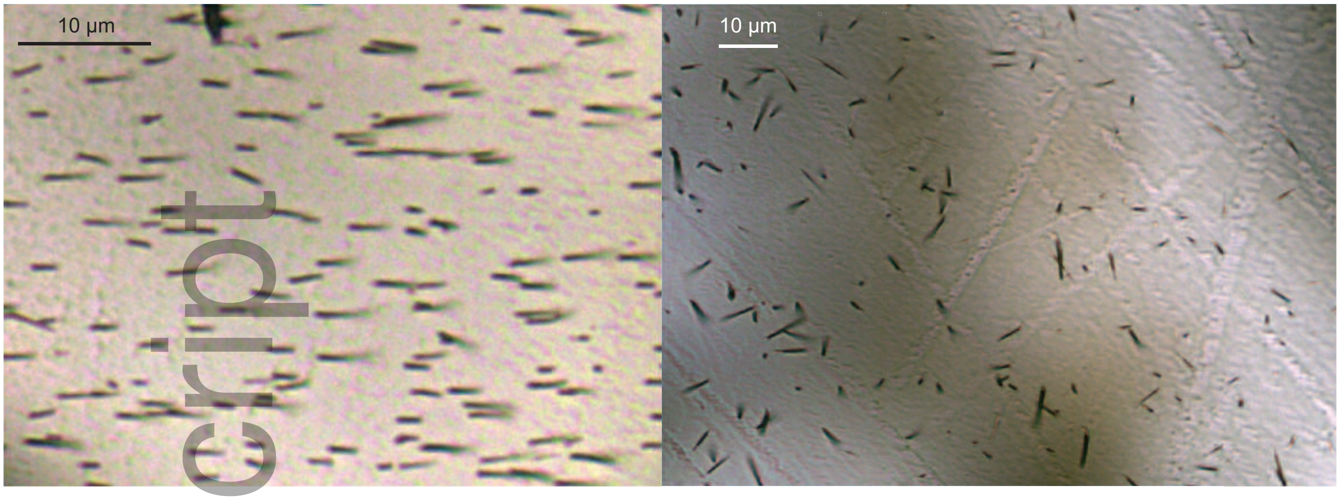

10 μm
10 μm


c)

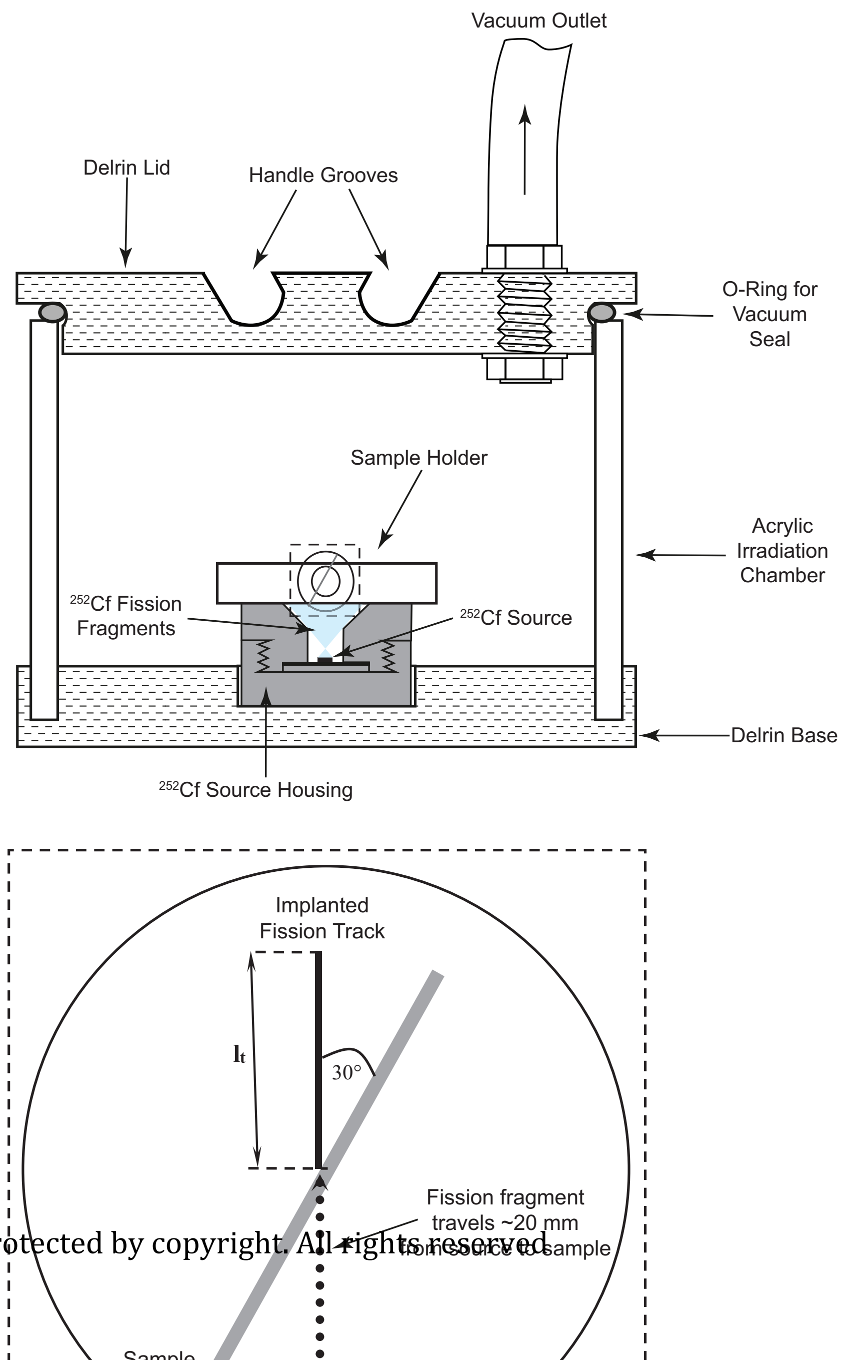

Vacuum Outlet
Delrin Lid
Handle Grooves
O-Ring for Vacuum Seal
Sample Holder
Acrylic Irradiation Chamber
252Cf Fission Fragments
252Cf Source
Delrin Base
252Cf Source Housing
Implanted Fission Track
lt
30°
Fission fragment travels ~20 mm from source to sample

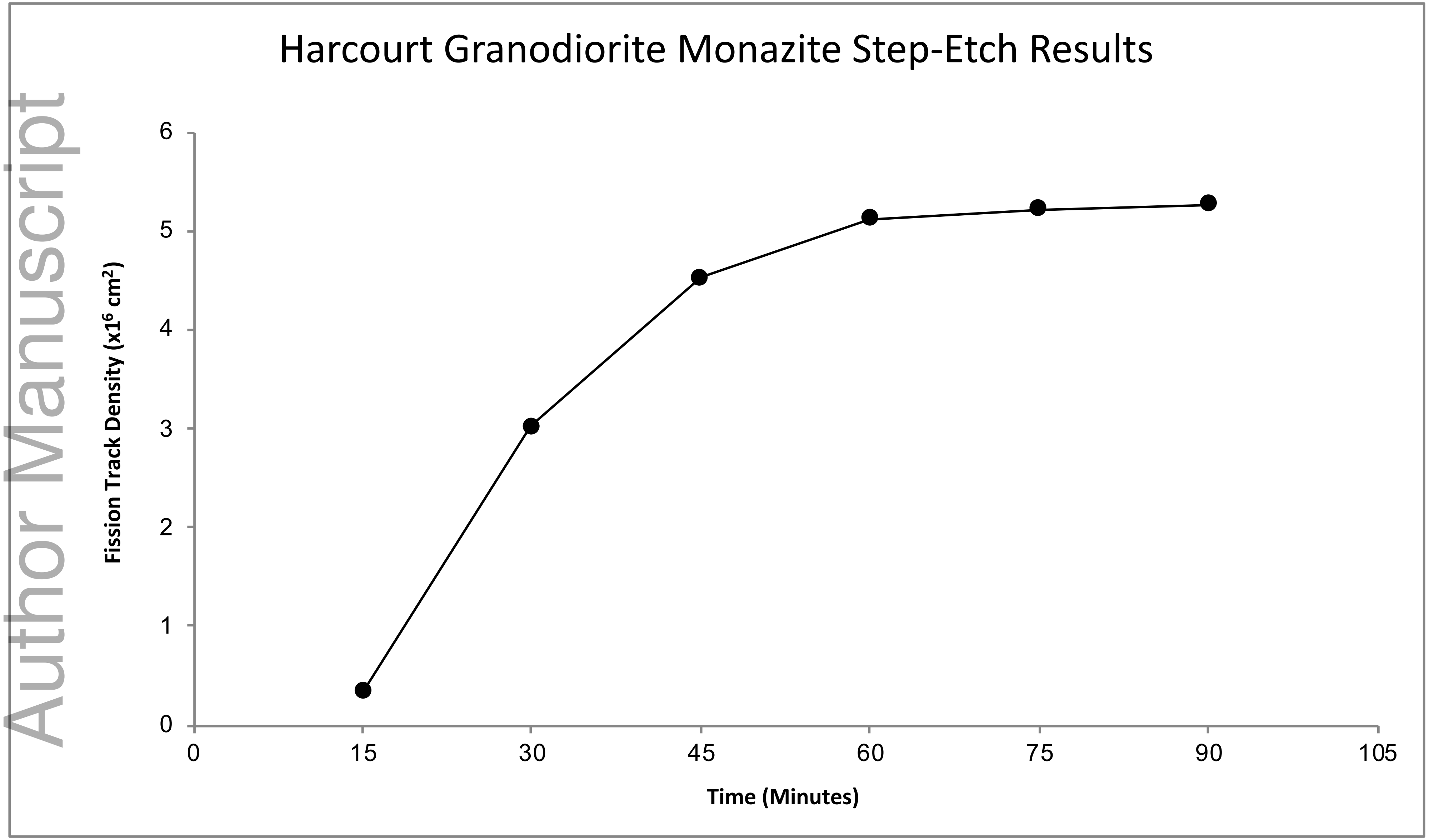
Harcourt Granodiorite Monazite Step-Etch Results
Fission Track Density (x1$^{6}$ cm$^{2}$)
6
5
4
3
2
1
0
0
15
30
45
60
75
90
105
Time (Minutes)

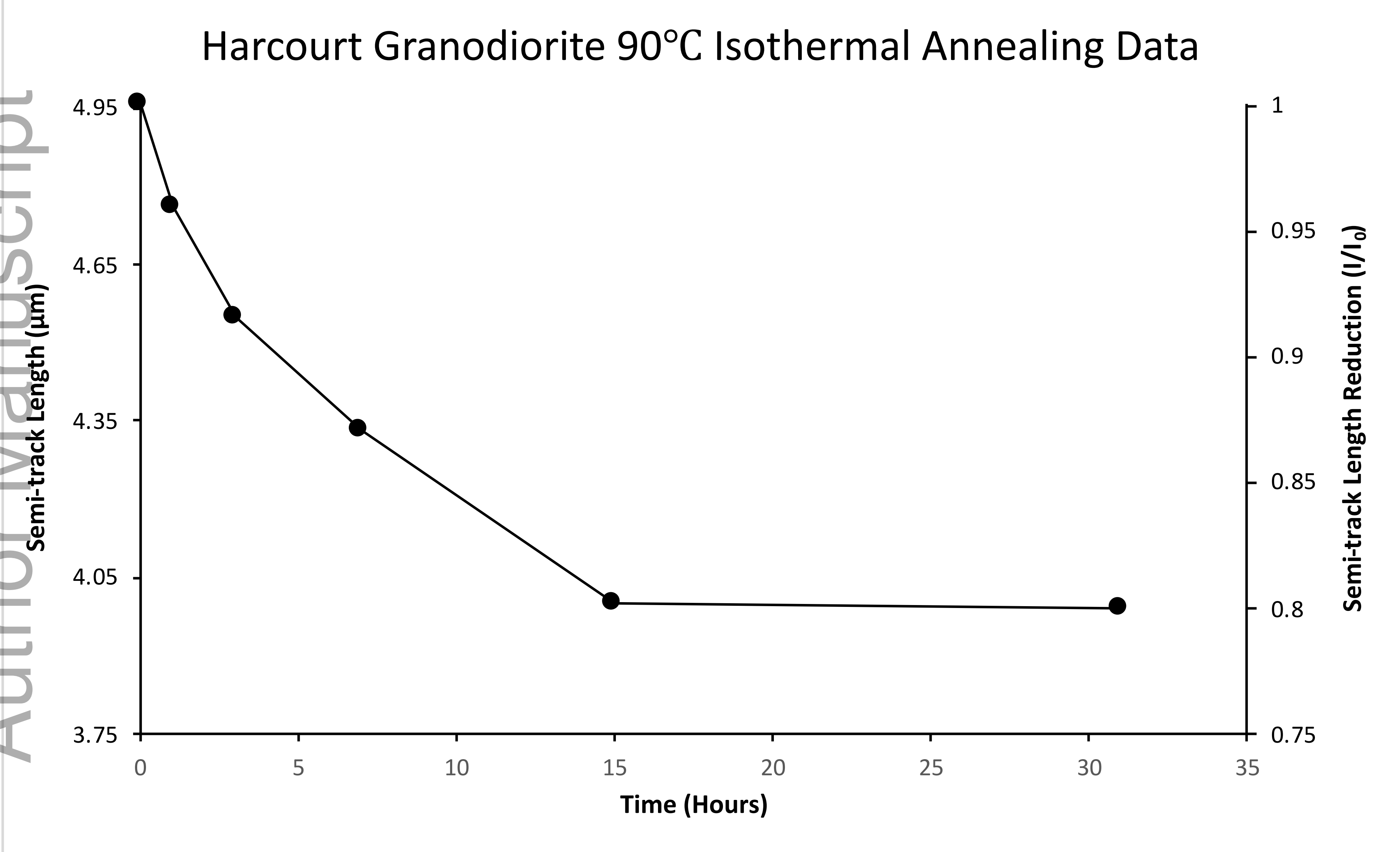
Harcourt Granodiorite 90°C Isothermal Annealing Data
Semi-track Length (µm)
4.95
4.65
4.35
4.05
3.75
Semi-track Length Reduction (l/l0)
1
0.95
0.9
0.85
0.8
0.75
0
5
10
15
20
25
30
35
Time (Hours)